Structure of Colloidal Gels during Microchannel Flow

Jacinta C. Conrad[†,‡] and Jennifer A. Lewis*[,†,‡,§]

Frederick Seitz Materials Research Laboratory, Materials Science and Engineering Department, and Chemical and Biomolecular Engineering Department, University of Illinois, Urbana, Illinois 61801

Received March 24, 2008. Revised Manuscript Received June 5, 2008

We investigate the structure and flow behavior of colloidal gels in microchannels using confocal microscopy. Silica particles are first coated with a cationic polyelectrolyte and then flocculated by the addition of an anionic polyelectrolyte. In the quiescent state, the suspension is an isotropic and homogeneous gel. Under shear flow, the suspension contains dense clusters that yield at intercluster boundaries, resulting in network breakup at high shear rates. These structural changes coincide with a transition from pluglike flow at low pressures to fluidlike flow at high pressures.

Introduction

Flow modifies the structure of attractive colloidal suspensions because of the competition between interparticle and hydrodynamic forces.[1] Attractive interactions between particles induce gelation, whereas flow-induced hydrodynamic forces disrupt the gel network.[2] Thus, attractive suspensions continually break up and reaggregate under shear flow,[3] which is correlated with changes in rheological behavior.[4] Although flow-induced restructuring has been extensively investigated with video microscopy and scattering for simple shear flows in bulk geometries,[5−8] the effects of confinement on restructuring are not well understood. For example, the high surface-area-to-volume ratio of microchannels may exacerbate the effects of wall slip,[9] and the formation of transient stress chains at constrictions may cause intermittent jamming of concentrated suspensions.[10] Despite its relevance to many applications, including microextrusion,[11−13] microfluidic assembly,[14,15] and direct-write assembly,[16] the structure of flowing attractive suspensions has not been studied in microchannel geometries.

Direct visualization techniques enable in situ investigations of the flow of colloidal suspensions in confined geometries. For example, fluorescence correlation spectroscopy (FCS) has been used to obtain particle velocities in dilute colloidal suspensions,[17] and microparticle imaging velocimetry (μ-PIV)[18,19] has been used to determine the flow profiles of hydrophobic colloidal gels as a function of flow rate.[20] However, neither FCS nor μ-PIV can be used to probe flow-induced restructuring directly because the individual colloids that constitute the gel network are not imaged in these techniques. By contrast, confocal laser scanning microscopy (CSLM) allows direct visualization of both the local and long-range structure of colloidal gels.[21−24] With scan speeds of ∼100 frames/s, fast-scanning confocal microscopes are well suited for in situ flow experiments under an applied shear stress. Although CSLM has been used to investigate the flow behavior of both hard-sphere colloidal fluids[25] and glasses[26,27] in microchannels, it has yet to be applied to the study the shear flow of attractive suspensions in similar geometries.

In this letter, we investigate the flow of attractive colloidal suspensions through microchannels using confocal microscopy. We induce attractions between silica particles via polymer bridging and directly image the suspensions under quiescent and shear flow conditions. The bulk structure of the quiescent suspension is a nearly isotropic, nonfractal network. When the suspension is flowed through a microchannel, the viscous stresses exerted during flow disrupt the gel network. Moreover, the flow also changes the structure of the clusters, which become more compact relative to the quiescent state. Yielding during microchannel flow occurs as interconnected clusters break apart near the walls, where the shear stress is highest. Accompanying these structural changes are qualitative changes in the flow behavior. Bulk rheological measurements indicate that these suspensions are highly shear thinning and exhibit a yield stress above which flow occurs. Additionally, the shape of the flow profile in the

* Corresponding author. E-mail: jalewis@uiuc.edu.
† Frederick Seitz Materials Research Laboratory.
‡ Materials Science and Engineering Department.
§ Chemical and Biomolecular Engineering Department.

(1) Vermant, J.; Solomon, M. J. *J. Phys.: Condens. Matter* **2005**, *17*, R187–R216.
(2) Tolpekin, V. A.; Duits, M. H. G.; van den Ende, D.; Mellema, J. *Langmuir* **2004**, *20*, 2614–2627.
(3) Hunter, R. J.; Frayne, J. *J. Colloid Interface Sci.* **1980**, *76*, 107–115.
(4) Varadan, P.; Solomon, M. J. *J. Rheol.* **2003**, *47*, 943–968.
(5) Degroot, J. V.; Macosko, C. W.; Kume, T.; Hashimoto, T. *J. Colloid Interface Sci.* **1994**, *166*, 404–413.
(6) Verduin, H.; deGans, B. J.; Dhont, J. K. G. *Langmuir* **1996**, *12*, 2947–2955.
(7) Hoekstra, H.; Vermant, J.; Mewis, J. *Langmuir* **2003**, *19*, 9134–9141.
(8) Hoekstra, H.; Mewis, J.; Narayanan, T.; Vermant, J. *Langmuir* **2005**, *21*, 11017–11025.
(9) Smay, J. E.; Gratson, G. M.; Shepherd, R. F.; Cesarano, J., III; Lewis, J. A. *Adv. Mater.* **2002**, *14*, 1279–1283.
(10) Haw, M. D. *Phys. Rev. Lett.* **2004**, *92*, 185506.
(11) Heule, M.; Vuillemin, S.; Gauckler, L. J. *Adv. Mater.* **2003**, *15*, 1237–1245.
(12) Rao, R. B.; Krafcik, K. L.; Morales, A. M.; Lewis, J. A. *Adv. Mater.* **2005**, *17*, 289–293.
(13) Wang, J. W.; Shaw, L. L.; Cameron, T. B. *J. Am. Ceram. Soc.* **2006**, *89*, 346–349.
(14) Yi, G.-R.; Thorsen, T.; Manoharan, V. N.; Hwang, M.-J.; Jeon, S.-J.; Pine, D. J.; Quake, S. R.; Yang, S.-M. *Adv. Mater.* **2003**, *15*, 1300–1304.
(15) Shepherd, R. F.; Conrad, J. C.; Rhodes, S. K.; Link, D. R.; Marquez, M.; Weitz, D. A.; Lewis, J. A. *Langmuir* **2006**, *22*, 8618–8622.
(16) Lewis, J. A. *Curr. Opin. Solid State Mater. Sci.* **2002**, *6*, 245–250.
(17) Hashmi, S. M.; Loewenberg, M.; Dufresne, E. R. *Opt. Express* **2007**, *15*, 6528–6533.
(18) Santiago, J. G.; Wereley, S. T.; Meinhart, C. D.; Beebe, D. J.; Adrian, R. J. *Exp. Fluids* **1998**, *25*, 316–319.
(19) Meinhart, C. D.; Wereley, S. T.; Santiago, J. G. *Exp. Fluids* **1999**, *27*, 414–419.
(20) Roberts, M. T.; Mohraz, A.; Christensen, K. T.; Lewis, J. A. *Langmuir* **2007**, *23*, 8726–8731.
(21) Dinsmore, A. D.; Weitz, D. A. *J. Phys.: Condens. Matter* **2002**, *14*, 7581–7597.
(22) Varadan, P.; Solomon, M. J. *Langmuir* **2003**, *19*, 509–512.
(23) Dibble, C. J.; Kogan, M.; Solomon, M. J. *Phys. Rev. E* **2006**, *74*, n/a.
(24) Prasad, V.; Semwogerere, D.; Weeks, E. R. *J. Phys.: Condens. Matter* **2007**, *19*, 113102.
(25) Frank, M.; Anderson, D.; Weeks, E. R.; Morris, J. F. *J. Fluid Mech.* **2003**, *493*, 363–378.
(26) Isa, L.; Besseling, R.; Weeks, E. R.; Poon, W. C. K. *J. Phys. Conf. Ser.* **2006**, *40*, 124–132.
(27) Isa, L.; Besseling, R.; Poon, W. C. K. *Phys. Rev. Lett.* **2007**, *98*, 198305.

10.1021/la800919k CCC: $40.75
Published on Web 06/27/2008

microchannel changes with applied pressure. At low applied pressures, the flow profile develops a region of nearly constant velocity approximating pluglike flow; as the applied pressure is increased, the flow becomes progressively more fluidlike. This qualitative change in the flow profiles can be related to the macroscopic suspension rheology: pluglike flow is observed when the estimated shear rate is in the shear-thinning regime, whereas fluidlike flow is observed when this shear rate lies within the high-shear plateau. These measurements provide insight into the effects of shear flow on the structure of attractive colloidal suspensions.

Experimental Methods

Materials System. Fluorescent-core silica microspheres are synthesized using a modified Stöber process.[28] The colloid diameter, d, is 824 ± 48 nm, as measured using scanning electron microscopy (6060LV, JEOL, Tokyo, Japan), and the density is 1.94 g/mL. After repeated washing in ethanol and in water at pH 6 to remove any excess reagents, the microspheres are suspended in pH 6 double-deionized water and diluted to a volume fraction of $\phi = 0.05$. A cationic polyelectrolyte, poly(ethyelenimine) (PEI, $M_w = 1800$, Polysciences, Inc., Warrington, PA), is added to the colloidal suspension at a ratio of 2.5 mg PEI/m^2 of silica. After PEI adsorption, the zeta potential of the coated microspheres suspended in double-deionized water at pH 6 is 46 ± 2 mV. To match the refractive index, the microspheres are suspended in a 65:35 v/v solution of dimethylsulfoxide (DMSO, Fisher Chemical, Fairlawn, NJ) and pH 6 double-deionized water ($\rho_{DMSO\text{-}H_2O} = 1.084$ g/mL) and then concentrated by sedimentation to an appropriate volume fraction. To induce an attraction between the PEI-coated microspheres, an anionic polyelectrolyte, poly(acrylic acid) (PAA, M_w=2000, Aldrich Chemical, St. Louis, MO), is added in a ratio of 2:1 [COONa]/[NH_x] ionizable charge groups. The PAA solution is added in four aliquots to the suspension, which is vortex mixed for ~1 s after each addition.

Confocal Microscopy. The structure of both quiescent and flowing suspensions is characterized using confocal microscopy. All images are acquired with a Vt-eye confocal (Visitech, Sunderland, U.K.) attachment on an Olympus microscope with a 100× objective lens (N.A. = 1.32). To determine the bulk quiescent structure of the suspensions, we acquire 3D image stacks in large sample chambers; the frame rate for a 2D image is ~2 frames/s, and the vertical spacing between consecutive images is 0.1 μm. To fabricate microchannel devices for the flow experiments, polyethylene tubing (Intramedic PE10, BD, Franklin Lakes, NJ) with an inner diameter of 0.28 mm is affixed to the ends of a glass microcapillary with inner dimensions of 50 μm × 50 μm and a length of 50 mm (Vitrocom, Mountain Lakes, NJ). The lengths of the input and output tubing are 15 and 6.5 cm, respectively. To drive the flow of the colloidal suspension through the microchannel, a pressure is applied across the device via a custom-built pressure box. For the experiments discussed herein, the minimum and maximum applied pressures are 0.69 and 10 kPa, respectively. The silica microspheres are directly imaged during flow at the midpoint along the length of the glass microcapillary. The high particle velocities observed during flow at even the lowest applied pressures preclude 3D imaging of individual colloids; thus, we acquire 2D images at a frame rate of 140 frames/s. At each pressure, 1000 images are taken at heights ranging from 3 to 30 μm above the bottom surface of the microchannel. For $\phi \geq 0.30$, clogging frequently disrupts the suspension flow within the microchannel even at the highest applicable pressures. We therefore restrict our detailed studies of the flow to the suspension with $\phi = 0.27$.

Image Analysis. The 2D images acquired during flow are analyzed using routines written in IDL (ITT Corporation, Boulder, CO). To obtain information about the spatial arrangement of particles during flow, we use standard algorithms to locate the positions of the particles in two dimensions.[29] By averaging over all images, we calculate the distribution of Voronoi areas; particles near the edges of the images with a large area are discarded. We define two particles to have a nearest-neighbor bond when the separation between them is greater than the particle diameter and less than the first minimum in the 2D radial distribution function. A cluster is then defined as the set of particles that are connected by nearest-neighbor bonds in two dimensions. We calculate the distribution of the number of nearest-neighbor bonds per particle and the distribution of the number of particles in a cluster, again averaging over all images. The colloidal microspheres in our experiments move distances greater than the interparticle separation in consecutive frames, and thus standard algorithms for tracking the positions of the particles cannot be used. Instead, the advection velocity across the microchannel is calculated using an alternate algorithm inspired by one used to analyze images of flowing colloidal glasses.[26,27] Briefly, each image is subdivided into vertical slices (of constant x, along the flow direction y) in which the velocity is uniform. For each pair of consecutive images $I_1(x, y)$ and $I_2(x, y)$, each slice in the latter image is shifted along the flow direction by a factor Δy chosen to maximize the cross-covariance between $I_1(x, y)$ and $I_2(x, y + \Delta y)$. For each vertical slice of constant x, the histogram of shifts Δy over the entire image series exhibits a sharp maximum. We fit this histogram with a Gaussian and report the position of the center of the Gaussian as the advection velocity at the horizontal position x. This 2D analysis, which is necessitated by the high particle velocities, may obscure features of the 3D structure. Hence, for the quiescent samples, we also locate the particle positions in three dimensions and calculate the distribution of Voronoi volumes and the distribution of the number of bonds per particle in three dimensions.

Rheological Measurements. The rheological properties of the colloidal suspensions are measured with a controlled-stress rheometer (C-VOR, Malvern Instruments, Southborough, MA). We perform both oscillatory and steady-shear measurements. To minimize wall slip, measurements are performed using a six-bladed vane tool (14 mm) in conjunction with a splined 15.4-mm cup. Prior to all rheological measurements, samples are sonicated for 1 min with a 1s on/off pulse. Between measurements, samples are first sheared for 60 s at a steady shear rate of 100 s^{-1} to reinitialize the shear history. Samples are then allowed to age for 2400 s to allow long-range structures to form. The apparent viscosity of the suspension, η, and the stress, σ, are measured as a function of the steady shear rate, $\dot{\gamma}$, over the range of 0.1−200 s^{-1}. We fit the viscometry data to the Herschel−Bulkley model,[30] $\sigma = \sigma_y + k\dot{\gamma}^n$, using the nonlinear curve-fitting routines in Kaleidagraph (Synergy Software, Reading, PA). The elastic (G') and viscous (G'') moduli are measured as functions of the applied stress, σ, over the range of 0.1−50 Pa at a frequency of 1 Hz.

Finite-Element Modeling. We calculate the flow profiles expected for a Herschel−Bulkley fluid using the finite-element method.[20,31,32] We solve the 1D momentum conservation equation in rectilinear geometry,[33,34] $\partial P/\partial z = \partial(\eta\partial U/\partial x)/\partial x + \partial(\eta\partial U/\partial y)/\partial y$, where $\partial P/\partial z$ is the pressure drop along the channel, $U = U(x, y)$ is the flow velocity, and $\eta = \eta(\dot{\gamma})$ is the viscosity, using COMSOL Multiphysics (COMSOL, Burlington, MA). Explicitly, $\eta = \sigma_y/[(\partial U/\partial x)^2 + (\partial U/\partial y)^2]^{1/2} + k[(\partial U/\partial x)^2 + (\partial U/\partial y)^2]^{(n-1)/2}$, where σ_y, k, and n are the parameters obtained from the fit of the viscometry data to the Herschel−Bulkley model. We model one-quarter of the cross section of a square channel with side length 50 μm using no-slip boundary conditions at the outer walls and symmetric boundary conditions at the center of the channel. The pressure gradient along the device is difficult to determine because of the change in diameter between the tubing and the microchannel. Instead, for each applied pressure we

(28) van Blaaderen, A.; Vrij, A. *Langmuir* **1992**, *8*, 2921–2931.
(29) Crocker, J. C.; Grier, D. G. *J. Colloid Interface Sci.* **1996**, *179*, 298–310.
(30) Bulkley, W. H.; Herschel, A. R. *Kolloid Z.* **1926**, *39*, 291–300.
(31) Alexandrou, A. N.; McGilvreay, T. M.; Burgos, G. *J. Non-Newton. Fluid Mech.* **2001**, *100*, 77–96.
(32) Burgos, G. R.; Alexandrou, A. N. *J. Rheol.* **1999**, *43*, 463–483.
(33) Batchelor, G. K. *An Introduction to Fluid Dynamics*; Cambridge University Press: Cambridge, U.K., 2000.
(34) Syrjala, S. *International Communications in Heat and Mass Transfer* **1995**, *22*, 549–557.

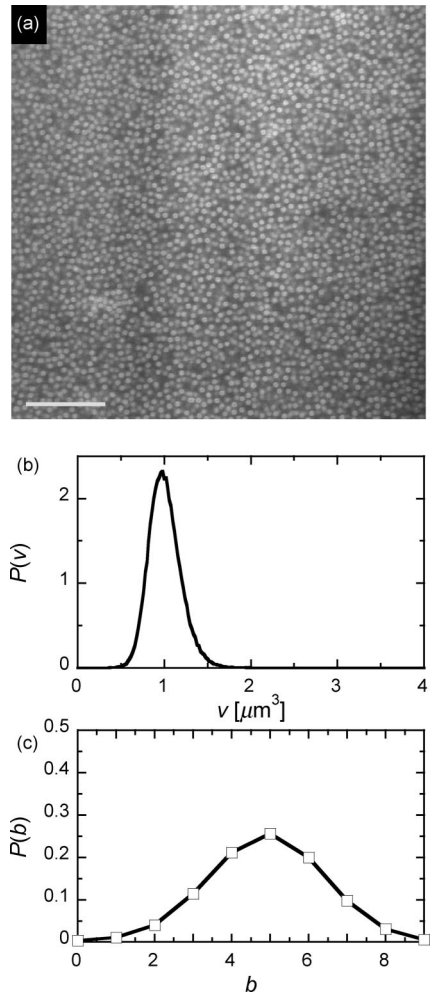

Figure 1. (a) Confocal micrograph ($x-y$ plane) of a quiescent colloidal gel with $\phi = 0.27$ acquired at a height of 12 μm above the bottom of the sample. The scale bar is 10 μm. (b) Distribution of Voronoi volume, v, and (c) distribution of the number of bonds per particle, b, calculated from 3D images of the quiescent sample.

find the value of the pressure gradient for which the maximum predicted flow velocity equals the maximum measured experimental flow velocity. We then compare the flow profile at that pressure gradient to the experimental flow profile at that applied pressure.

Results and Discussion

In a quiescent sample at $\phi = 0.27$, the colloidal particles form a static, space-spanning gel with a nearly isotropic structure, as shown in Figure 1. The distribution of Voronoi volumes, $P(v)$, is sharply peaked, and the distribution of the number of bonds per particle, $P(b)$, confirms that all particles are connected to the gel network. The morphology seen here is reminiscent of that observed in depletion gels with a short-range interaction[35] whose strength is on the order of tens of k_BT.[23]

Flow disrupts the gel network and can lead to restructuring of the colloidal clusters. In our experiments, the magnitude of the applied pressure determines the extent of disruption. Flow under small applied pressures drives restructuring within the gel, as shown in the confocal micrographs in Figure 2a−e for an applied pressure of 0.69 kPa. In sharp contrast to the isotropic network morphology seen in the quiescent state (Figure 1), the suspension flowing under a small applied pressure contains distinct, dense clusters. Yielding near the wall occurs via the disruption of these clusters at the weak points connecting them to the gel network. (See Supporting Information for movies of the flow.) The locally dense clusters rotate when yielding because of the horizontal gradient in the local shear environment. The presence of these clusters indicates that the gel structure is not completely disrupted by the flow under modest shear.

Flow driven by a large applied pressure completely disrupts the gel network, as shown by the confocal micrographs in Figure 2f−j for an applied pressure of 10 kPa. Near the bottom wall of the channel, where the shear stress is highest, the network appears to be almost completely broken into individual particles or small clusters (Figure 2j). This disruption persists even near the midplane of the microchannel (Figure 2f). We note that imaging is difficult at these high applied pressures; the particle velocities ($\sim$2 mm/s) are essentially at the limit resolvable with CSLM, resulting in significant distortions in the particle images.

To quantify the structural changes in the gel network induced by the flow, we first calculate the distribution of two-dimensional Voronoi areas, $P(a)$. For the quiescent sample shown in Figure 1, $P(a)$ contains a sharp maximum, indicating that the gel structure is relatively uniform (Figure 3a). By contrast, the width of $P(a)$ for a sample flowing under an applied pressure of 0.69 kPa is much broader than that of the quiescent sample. As the applied pressure is further increased, the width of this distribution also increases; however, at the highest pressures, this increase arises in part from the distortions caused by the high flow speeds. These changes indicate that the structure of the suspensions during flow is significantly more heterogeneous than in the quiescent state.

We further characterize the change in local structure by calculating the 2D distribution of the number of bonds per particle, $P(b)$. For the quiescent sample, $P(b)$ is strongly peaked near $b \approx 3$, as shown in Figure 3b. When the suspension flows under an applied pressure of 0.69 kPa, the position of the peak shifts to lower b, showing that the overall number of bonds per particle decreases. However, $P(b)$ also displays a tail at higher values of b, showing that some particles maintain a higher coordination number. When the applied pressure is further increased, most particles have either zero or one bond; concomitantly, the number of particles in the high-b tail of the distribution decreases. These changes in $P(b)$ suggest that the gel network is first broken into clusters at low applied pressures and then further divided into individual particles at the highest applied pressures. We confirm these ideas by calculating the distribution of the number of particles in a cluster, $P(n)$. For the quiescent sample, all particles are connected and form a single system-spanning cluster in three dimensions. By contrast, for a suspension flowing under an applied pressure of 0.69 kPa, we observe relatively few large clusters, as shown in Figure 3c. Instead, $P(n)$ increases at low values of n, indicating that the flow disrupts the network and breaks it into smaller clusters. As the applied pressure is increased to 10 kPa, the number of large clusters further decreases; concomitantly, the number of particles with no neighbors increases. The high particle velocities preclude 3D imaging during flow, and thus we cannot ascertain whether connections between clusters exist out-of-plane. Nevertheless, the decrease in the number of large clusters and the accompanying increase in the number of particles with no nearest-neighbor bonds confirm that the degree of network disruption increases with increasing applied pressure.

The morphological changes observed with direct imaging are reflected in the rheological behavior. Colloidal suspensions with a bridging interaction are strongly shear-thinning, as shown in Figure 4a. In the range of volume fractions studied ($0.27 \leq \phi$

(35) Lu, P. J.; Conrad, J. C.; Wyss, H. M.; Schofield, A. B.; Weitz, D. A. *Phys. Rev. Lett.* **2006**, *96*, 4.

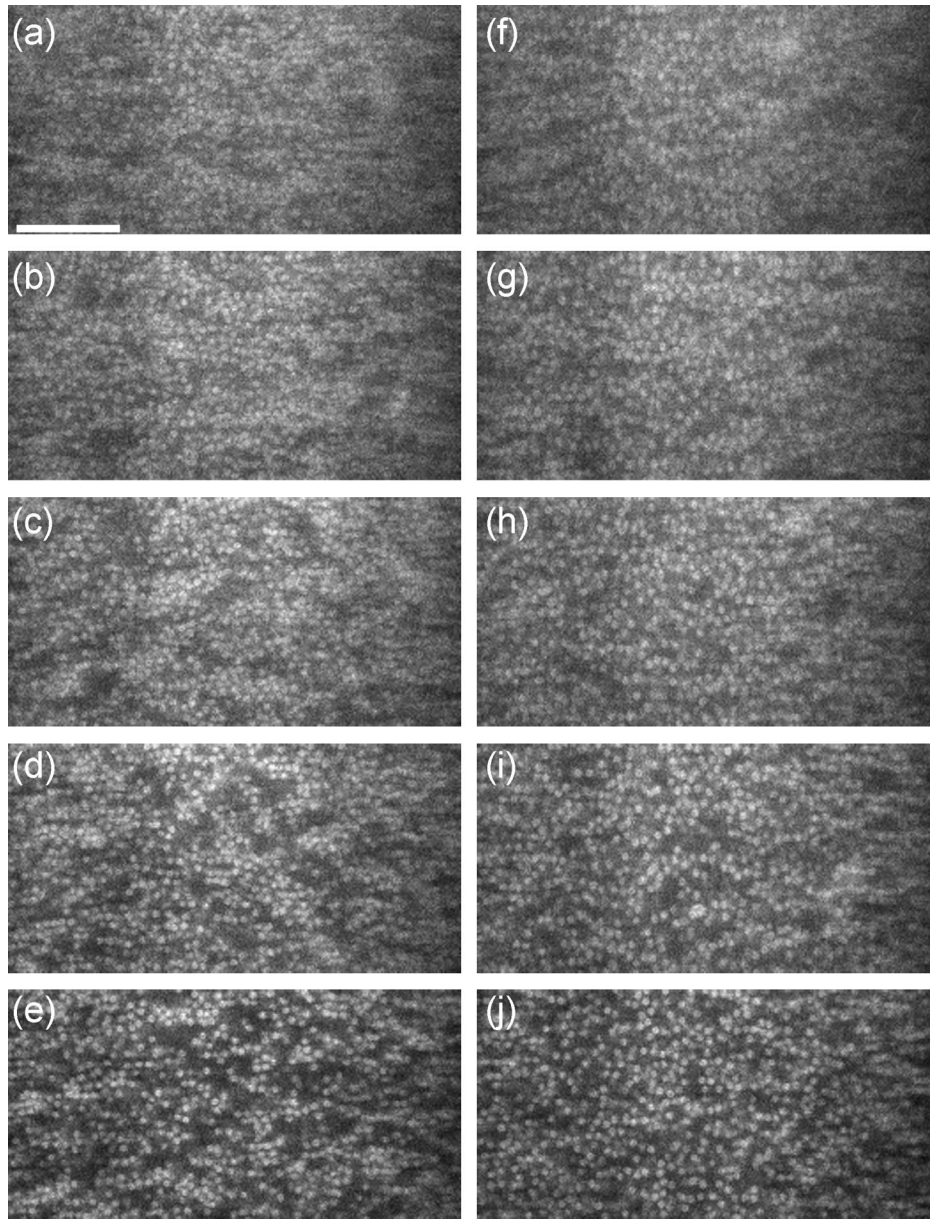

Figure 2. Confocal micrographs of a colloidal gel with $\phi = 0.27$ flowing under applied pressures of (a−e) $\Delta P = 0.69$ kPa and (f−j) $\Delta P = 10$ kPa at different heights above the bottom of the microchannel. (a, f) 15 μm, (b, g) 12 μm, (c, h) 9 μm, (d, i) 6 μm, and (e, j) 3 μm. Flow is in the downward vertical direction. The scale bar is 10 μm.

≤ 0.34), the apparent viscosity, η, is highest at the lowest shear rates measured, $\dot{\gamma} = 0.1\ s^{-1}$ and decreases with increasing shear rate until $\dot{\gamma} \approx 10\ s^{-1}$. When $\dot{\gamma} > 10\ s^{-1}$, η is nearly independent of shear rate, indicating that at sufficiently high $\dot{\gamma}$ the suspension flows freely and is liquidlike. The change in the high-shear plateau viscosity over this volume fraction range is much larger than that expected for a fluid of spheres, as determined from the Krieger−Dougherty equation,[36] $\eta = \eta_0(1 - \phi/\phi_m)^{-[\eta]\phi_m}$, where η_0 is the viscosity of the suspending fluid, $\phi_m = 0.68$ as reported in an earlier study on the viscosity of suspensions of hard-sphere colloids at high shear rates,[37] and $[\eta] = 2.5$ is the intrinsic viscosity. The failure of this scaling confirms our observation from microscopy that the network is not completely broken into individual particles. The shear stress approaches a constant value at low shear rates, as shown in the inset to Figure 4a. We therefore fit the stress data obtained from the viscometry measurements to the Herschel−Bulkley model,[30] $\sigma = \sigma_y + k\dot{\gamma}^n$, as indicated by the dotted lines.

The colloidal gels behave like weak viscoelastic solids when ϕ is sufficiently high. When the applied stress, σ, is small, the elastic modulus is larger than the viscous modulus, $G' > G''$, and the value of G' is nearly independent of σ, as shown in Figure 4b. The existence of this plateau modulus, G'_p, is one key indicator of solidlike behavior. When σ is increased, the value of the elastic modulus precipitously drops, indicating that the gel network is disrupted. We define the yield stress, σ_y, as the value of the shear stress where $G' = 0.9G'_p$. Over the narrow range of ϕ studied, both σ_y and G'_p exhibit a power-law dependence upon ϕ, with $\sigma_y \approx \sigma^8$ and $G'_p \approx \phi$.[17] These exponents are significantly higher than those typically measured for colloidal gels.[38–41] We

(36) Krieger, I. M.; Dougherty, T. J. *Trans. Soc. Rheol.* **1959**, *3*, 137–152.
(37) Krieger, I. M. *Adv. Colloid Interfac.* **1972**, *3*, 111–136.
(38) Buscall, R.; Mills, P. D. A.; Goodwin, J. W.; Lawson, D. W. *J. Chem. Soc., Faraday Trans.* **1988**, *84*, 4249–4260.
(39) Shih, W. H.; Shih, W. Y.; Kim, S. I.; Liu, J.; Aksay, I. A. *Phys. Rev. A* **1990**, *42*, 4772–4779.

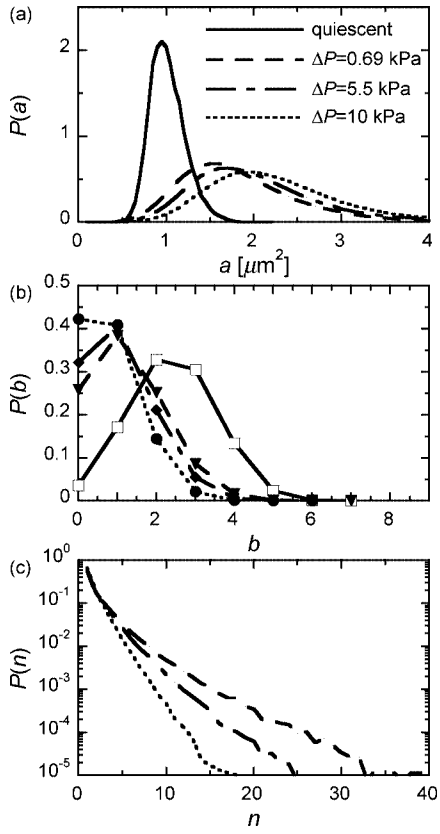

Figure 3. (a) Distribution of Voronoi area, a, (b) distribution of the number of bonds per particle, b, and (c) distribution of the number of particles in a cluster, n, for a colloidal gel with $\phi = 0.27$, as calculated from 2D images taken 12 μm above the bottom surface of the microchannel. Solid line, quiescent gel; dashed line, $\Delta P = 0.69$ kPa; dashed−dotted line, $\Delta P = 5.5$ kPa; and dotted line, $\Delta P = 10$ kPa. For the quiescent gel in panel c, the majority of particles belong to clusters with $n > 40$; therefore, the solid line is omitted.

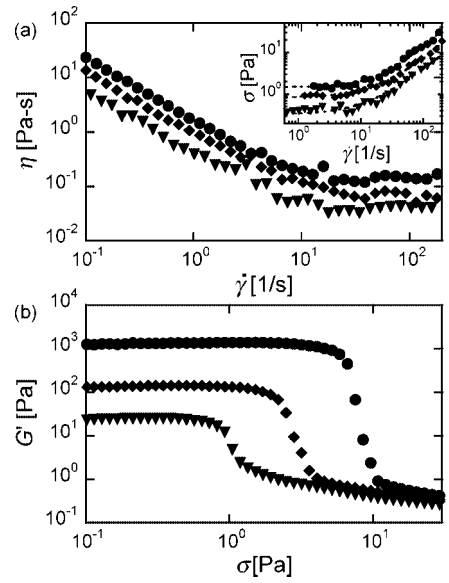

Figure 4. Rheological properties of colloidal gels. (a) Apparent viscosity, η, as a function of shear rate, $\dot{\gamma}$. (Inset) Shear stress, σ, as a function of $\dot{\gamma}$. (b) Elastic modulus, G', as a function of shear stress, σ, measured at a frequency of 1 Hz. Volume fractions: (●) $\phi = 0.34$, (♦) $\phi = 0.30$, and (▼) $\phi = 0.27$. The dotted lines in the inset to panel a are fits to the Herschel−Bulkley model.

tentatively suggest that these exponents may reflect the relatively weak attraction between colloids as well as the homogeneity of the gel network. We further confirm that these suspensions behave like weak solids by measuring the frequency-dependent linear viscoelastic moduli. Over two decades in frequency, we find $G' > G''$, again consistent with solidlike behavior. Furthermore, the linear elastic and viscous moduli exhibit a weak frequency dependence (not shown), $G', G'' \approx \omega^{0.2}$, as also seen in other soft solids.[42,43] When $\phi < 0.27$, we are unable to measure an elastic modulus, which suggests that any network formed at lower ϕ is too weak to support even small stresses.

To relate the macroscopic rheological behavior to the microscopic flow behavior, we calculate the advection velocity across the microchannel. When the applied pressure is relatively low (0.69 kPa), the advection velocity for a suspension with $\phi = 0.27$ is nearly constant across the width of the channel, as shown in Figure 5a. For each applied pressure, we rescale the velocities by the maximum velocity found for the data at a height of 18 μm. For comparison, we also calculate the normalized flow profile for a Newtonian fluid in a square channel at a height of 18 μm,[44] $U/U_{max} \propto \Sigma_{n\ \mathrm{odd}} (-1)^{(n-1)/2}[1 - \cosh(n\pi z/2L/\cosh(n\pi/2)]\cos(n\pi y/2L)/n^3$, where L is the half-width of the channel. The pluglike flow profile observed at an applied pressure of 0.69 kPa and a height of 18 μm deviates strongly from that expected for a Newtonian fluid; however, it is in reasonable agreement with that predicted by the Herschel−Bulkley model, as shown in Figure 6. Using the maximum velocity in the channel, we estimate the shear rate across the microchannel to be approximately 5 s^{-1}. At this value of $\dot{\gamma}$, the bulk viscometry measurements indicate that the suspension is strongly shear-thinning. When the applied pressure is increased to 5.5 kPa, the flow profile becomes more fluidlike (Figures 5b and 6); only near the center of the channel is the flow profile slightly flattened. At this applied pressure, the flow profile calculated using the Herschel−Bulkley model is nearly identical to that of the Newtonian fluid. We estimate the shear rate at this applied pressure to be $\dot{\gamma} \approx 34$ s^{-1}, just within the high-shear plateau region measured by bulk viscometry. When the applied pressure is further increased to 10 kPa, the shape of the velocity profile is very close to that expected for a Newtonian fluid, as shown in Figures 5c and 6. At this applied pressure, the estimated shear rate across the microchannel is $\dot{\gamma} \approx 120$ s^{-1}, well within the high-shear plateau measured by bulk viscometry. These measurements indicate that the onset of fluidlike flow occurs when the gel network is disrupted, i.e., when the local shear rate lies within the high-shear plateau. The relationship between the microscopic flow profile and the macroscopic viscosity described here is reminiscent of the "elastic floc" model,[45] which posits that the cluster deformation and rupture lead to significant energy dissipation during flow.

To parametrize the flow behavior of our colloidal gels in microchannels, we first determine the relative importance of advection and diffusion. Measurements of the 2D mean-square displacement of the quiescent gels show no appreciable increase over an experimental time of 1 h. Therefore, an upper bound for the diffusion constant is $D_0 = d^2/\tau$, with $\tau = 3600$ s. We estimate the minimum Péclet number to be $Pe = U_{min}L/D_0$, where $U_{min} \approx 150$ μm/s is the minimum velocity measured near the midplane of the channel. We find $Pe > 10^7$, clearly demonstrating that diffusion plays no role in the flow properties.

(40) Krall, A. H.; Weitz, D. A. *Phys. Rev. Lett.* **1998**, *80*, 778–781.
(41) Gisler, T.; Ball, R.; Weitz, D. A. *Phys. Rev. Lett.* **1999**, *82*, 1064–1067.
(42) Sollich, P.; Lequeux, F.; Hebraud, P.; Cates, M. E. *Phys. Rev. Lett.* **1997**, *78*, 2020–2023.
(43) Sollich, P. *Phys. Rev. E* **1998**, *58*, 738–759.
(44) White, F. M. *Viscous Fluid Flow*, 3rd ed.; McGraw-Hill: Boston, 2006.
(45) Firth, B. A.; Hunter, R. J. *J. Colloid Interface Sci.* **1976**, *57*, 266–275.

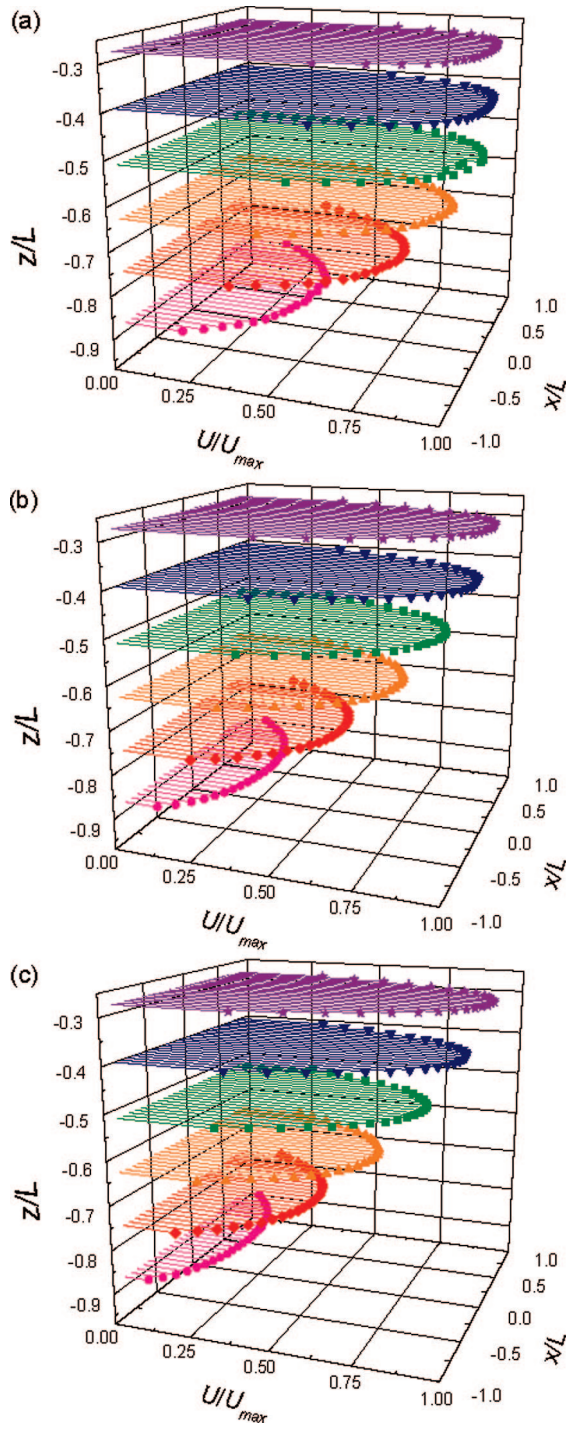

Figure 5. Flow profiles of a colloidal gel with $\phi = 0.27$. The applied pressure across the device is (a) $\Delta P = 0.69$ kPa, (b) $\Delta P = 5.5$ kPa, and (c) $\Delta P = 10$ kPa. Symbols indicate the height above the bottom of the microchannel: (●) 3, (◆) 6, (▲) 9, (■) 12, (▼) 15, and (★) 18 μm.

The relevant dimensionless parameter for the microchannel flow of colloidal gels is the Oldroyd number,[46] which is defined as the ratio of yield stress to viscous stress: $Od = \sigma_y/\sigma_v$.[47,48] We estimate the viscous stress using the constitutive model for a Herschel−Bulkley fluid: $\sigma_v = k(U/L)^n$, where U is the maximum advection velocity in the channel at that pressure, and $k = 0.0167$ and $n = 1.17$ are the Herschel−Bulkley parameters determined from the viscometry stress data in Figure 4a. For an applied pressure of 0.69 kPa, we estimate $Od \approx 2.7$, implying that the yield stress is significantly larger than the viscous stress. As the applied pressure is increased to 10 kPa, the Oldroyd number decreases to $Od \approx 0.091$, indicating that the viscous stress now dominates. Thus, the transition from pluglike to fluidlike flow occurs concomitantly with an increase in viscous stress imparted by the shear flow. The yield stress for these colloidal gels increases sharply with increasing ϕ; thus at comparable values of U, we also expect Od to increase dramatically with increasing ϕ. This implies that pluglike flow will persist at higher applied pressures in more concentrated gels undergoing microchannel flow.

(46) Huilgol, R. R.; You, Z. *J. Non-Newton. Fluid Mech.* **2005**, *128*, 126–143.
(47) Oldroyd, J. G. T. *Proc. Cambridge Philos. Soc.* **1947**, *43*, 100–105.
(48) Oldroyd, J. G. T. *Proc. Cambridge Philos. Soc.* **1947**, *43*, 383–395.

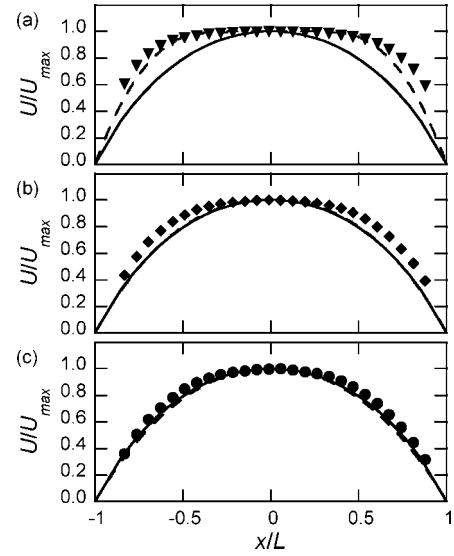

Figure 6. Flow profiles for a colloidal gel with $\phi = 0.27$ at a height of 18 μm above the bottom of the channel, at applied pressures of (a) (▼) $\Delta P = 0.69$ kPa, (b) (◆) $\Delta P = 5.5$ kPa, and (c) (●) $\Delta P = 10$ kPa. The solid line and the dotted line indicate the flow profiles expected for a Newtonian fluid and a Herschel−Bulkley fluid in a square microchannel, respectively.

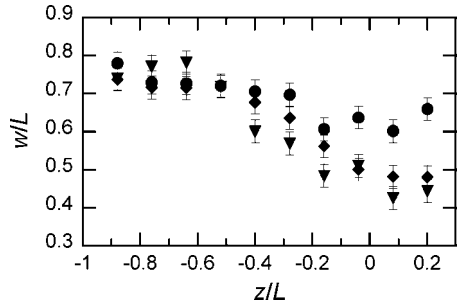

Figure 7. Normalized shear zone width, w/L, as a function of normalized height, z/L, for a colloidal gel with $\phi = 0.27$ with applied pressures of (▼) $\Delta P = 0.69$ kPa, (◆) $\Delta P = 5.5$ kPa, and (●) $\Delta P = 10$ kPa.

To quantify the change in the flow profiles as the applied pressure is increased, we calculate the shear zone width at different heights in the microchannel. For a given height, the shear zone width, w, is defined as the distance from the wall at which the advection velocity is equal to $0.95V_c$, where V_c is the maximum advection velocity at that height.[27] For an applied pressure of 0.69 kPa, $w \approx 0.72L \pm 0.03L$ near the channel walls and decreases to $\sim 0.42L$ near the center of the channel (Figure 7). When the applied pressure is increased, the variation of the shear zone width with height becomes less pronounced. For an applied pressure of 5.5 kPa, near the wall we again measure $w \approx 0.72L$; however, near the midplane of the microchannel, we find $w \approx 0.51L$. When the applied pressure is increased further to 10 kPa, the shear zone width near the midplane increases to $w \approx 0.63L$.

Thus, as the applied pressure is increased, the shear zone width also increases, consistent with the emergence of fluidlike flow.

Conclusions

We investigate the structure and flow profiles of attractive colloidal suspensions in microchannels with direct imaging. The isotropic network observed in quiescent samples is disrupted during shear flow. We show that the extent of this disruption is related to the applied pressure. Flow under small applied pressures drives the formation of compact clusters, whereas flow under larger applied pressures breaks the gel network into individual particles and small clusters. The microscopic flow profile can be directly connected to the shear-rate-dependent viscosity; the transition from pluglike to fluidlike flow occurs when the estimated shear rate across the microchannel exceeds the critical shear rate at which the onset of the high-shear plateau viscosity is observed. These results offer new insight into the relationship between flow behavior and mechanical properties in attractive colloidal suspensions.

Acknowledgment. This work was supported by the NSF Center for Directed Assembly of Nanostructures (grant no. DMR01-17792) and the NSF Center for Nanoscale Chemical-Electrical-Mechanical Manufacturing Systems (grant no. DMII-0328162). We gratefully acknowledge experimental suggestions from S. K. Rhodes and R. F. Shepherd, assistance with the finite-element modeling from C. J. Hansen and M. T. Roberts, and the use of software written by D. L. Blair to calculate the Voronoi distributions.

Supporting Information Available: Flowing gels in microchannels. This material is available free of charge via the Internet at http://pubs.acs.org.

LA800919K